

DESIGN AND CONSTRUCTION OF AN ACCURATE TIMING SINGLE CHANNEL ANALYZER*

A. EZZATPANAH LATIFI¹, F. ABBASI DAVANI^{1**},
M. SHAHRIARI¹ AND A. SHARGHI IDO²

¹Radiation Application Group, Faculty of Nuclear Engineering,
Shahid Beheshti University, Tehran, I. R. of Iran
Email: fabbasi@sbu.ac.ir

²Incubator Center of Technology Units of Shahid Beheshti University
P.O. Box: 1983963113, Tehran, I. R. of Iran

Abstract – In this paper we discuss an approach to the design and construction of an accurate timing single channel analyzer (TSCA) for the timing of pulses over a wide dynamic range. A brief overview of the timing methods and uncertainty factors as "walk and jitter" and a detailed description of the TSCA circuit are given together with some insight into the application and reasons that led us to the design and construction of constructed TSCA. The advantages of this instrument are then highlighted and the experimental results are presented.

Keywords – Timing Single Channel Analyzer (TSCA), Constant Fraction Trailing Edge (CFTE), Lower Level Discriminator (LLD), Upper Level Discriminator (ULD)

1. INTRODUCTION

The timing signal derivation and pulse height analysis of the nuclear detector output pulses are the most important functions that are needed in so many experiments, especially in the coincidence techniques [1], [2] and neutron-gamma separation [3]. The timing single channel analyzer unit (TSCA) performs the dual functions of single-channel pulse-height analysis and timing signal derivation. There are some error sources like walk and jitter and rise time variation of pulses that contribute to uncertainty in the timing measurement [4]. Some techniques are introduced for time characteristic derivation like the leading edge, cross over and constant fraction timing that are classified relative to the amount of timing uncertainty elimination [5]. After comparing these techniques, the constant fraction timing method for timing signal derivation was selected because it makes it possible to realize significant improvements in time resolution in most timing applications. This technique allows the optimization of the time resolution and the extension of the dynamic range for neutron-gamma discrimination and other timing applications. In addition to the choice of timing method, the design and implementation of such method is very important. In this work, we focused on designing and implementing an accurate and stable timing circuit based on the constant fraction trailing edge method. Finally, minimized timing uncertainties and precise pulse height analysis in were presented the results of some experiments that show the perfect performance of the constructed TSCA. A graphical picture of constructed TSCA is shown in Fig. 1.

*Received by the editor May 19, 2009 and in final revised form April 14, 2010

**Corresponding author

2. CIRCUIT DESCRIPTION

Low level noises and variation of input pulse amplitude cause a limitation of the effective dynamic range and degradation of the time resolution. Furthermore, the effect of time jitter that rises from the discrete nature of the electronic signal as generated in the detector, especially when the number of information carriers that make up the signal is low, causes time shift as an extra effect in the degradation of time resolution. So these observations led us to design an accurate timing system that eliminates timing uncertainties effects.



Fig. 1. graphical picture of constructed TSCA

The block diagram of constructed TSCA and the circuit diagram of each block are shown in Fig. 2 and Fig. 3. Unipolar or bipolar input pulses could be routed via DC or AC coupled inputs. The DC coupled routing makes it possible to take full advantage of the baseline restoration of the main amplifier for the maximum performance at widely varying counting rates. The LLD (Lower level discriminator) is a comparator that generates output when the leading edge of the input pulse triggers the lower level discriminator. The ULD (Upper level discriminator) acts similar to LLD. The LLD and ULD are employed as single channel pulse-height analysis.

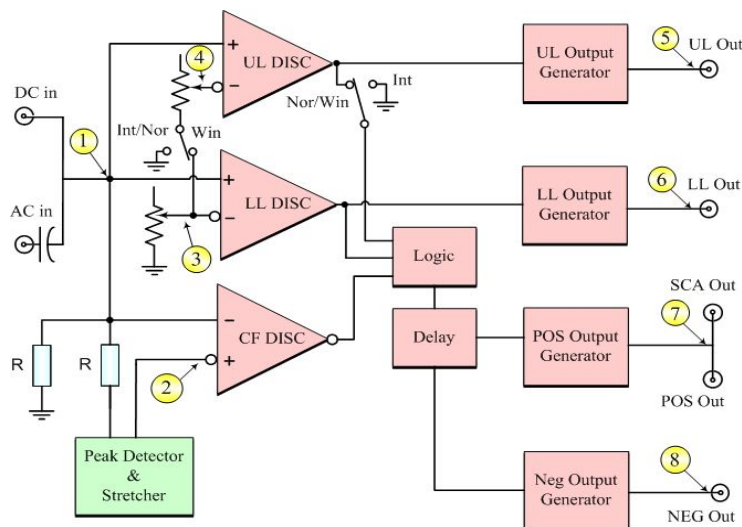


Fig. 2. Block diagram of constructed TSCA (Corresponding waveforms of measurement signs are shown in Fig. 5)

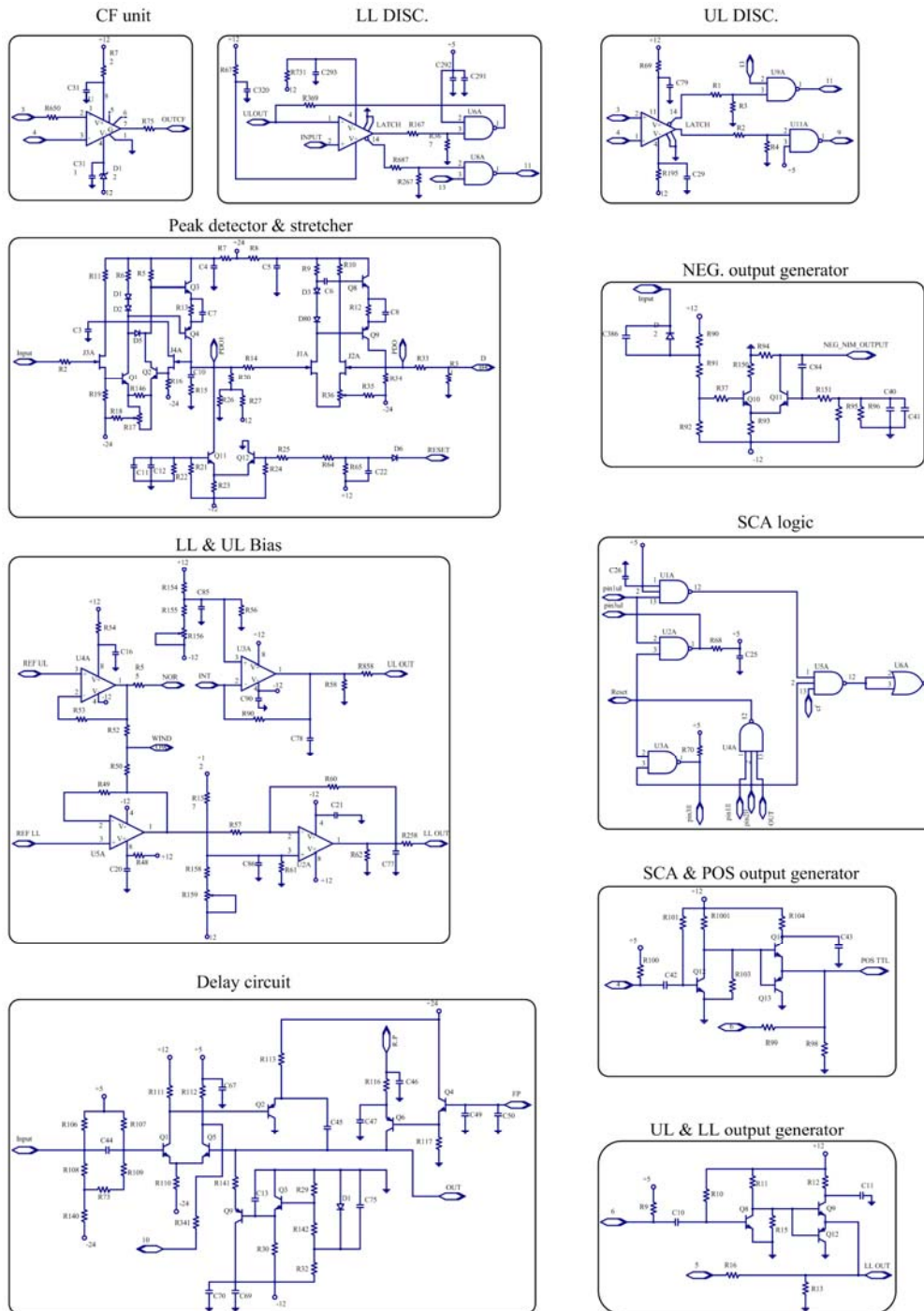


Fig. 3. Circuit diagrams of blocks of Fig. 2

The most important part of the TSCA circuit is the peak detection and stretch. The patented [6] trailing-edge constant fraction timing technique, which compensates for varying amplitudes and essentially eliminates this timing shift, giving consistently better timing results was selected. For the internally set 50% fraction, the output occurs soon after the midpoint on the linear input trailing edge to facilitate gating and the accumulation of data at very high input rates. This technique also minimizes the timing shift and dead time when used with sodium iodide, silicon, and germanium detectors, thereby allowing better time resolution at higher counting rates. Notice that analysis is made on the main amplifier output. This technique allows the optimization of time resolution and the extension of the dynamic range for time pick off applications.

As shown in Fig. 4, during the rise time of the input pulse the capacitor, C10, is charged. The reverse current is cut off, so the peak amplitude of the input pulse remains on C10 until the reset time. The peak amplitude of the input pulse is furnished through a unity buffer circuit. The walk adjust potentiometer provides a fine adjustment of the offset of this amplifier and is adjusted for its dynamic function to minimize walk in the time-significant output pulses. The detected peak, divided by 2, acts as a reference level in CFD (constant fraction discriminator). During the decay of the input pulse, its level drops down through the Constant fraction level at 50% of the peak amplitude, which is dependable and precise time in a shaped linear pulse. CFD then generate an output as a timing signal and reset the peak detection unit. The logic unit combines the three signals (LLD, ULD and CFD) mentioned above to generate the correct decision. For example, in window mode the logic output will be true (low) if and only if following condition is satisfied: when the amplitude of energy signal exceeds LLD but does not exceed ULD. (See the first and second waveforms in Fig. 5.)

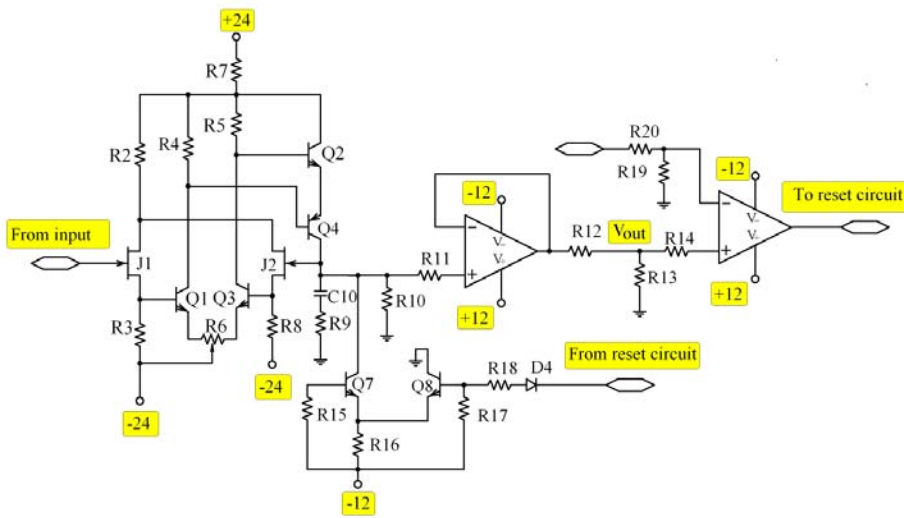


Fig. 4. Circuit diagram of Peak detect and stretch of constructed TSCA

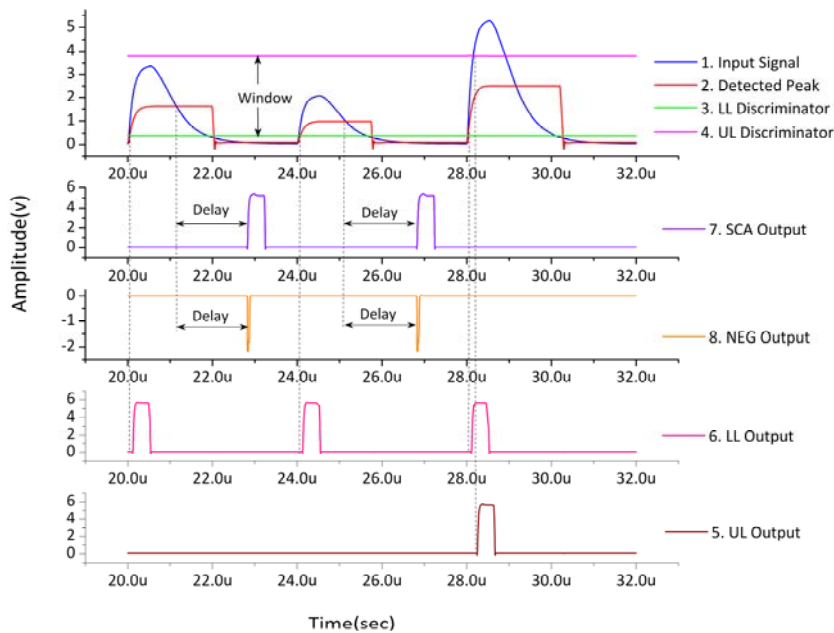


Fig. 5. Timing relationship between input and output of constructed TSCA (simulated by PSPICE software V10.0)

NEG output generator unit generates a fast negative NIM standard output with a rise time <5 ns and width <20 ns. POS output generator unit generates a slow positive NIM standard output with rise time <20 ns and width <500 ns. Minimum resolving time for negative output is 220 ns and for positive output is 800 ns. The relationships between the input, internal and output signals of TSCA are shown in Fig. 5. This Figure is simulated by PSPICE software [7].

3. RESULTS

In order to measure the time walk of constructed TSCA which defines its timing measurement performance, a set up shown in Fig. 6 was used.

In this set up the CFD unit measures a constant fraction of amplitude (about 10-20%) of every single pulse the pulser generates as a timing parameter in the leading edge. The output signal of CFD is delayed by the delay amplifier to be in coincidence with the other branch and sent to the TAC unit as a start signal. In the other branch the TSCA unit measures 50% of the pulse amplitude in the trailing edge as a timing parameter and sends it to the TAC unit as a stop signal. For obvious reasons the CFD signal is more stable than TSCA so that any variation in the MCA channels of the TAC output could be defined as a TSCA walk. Therefore, we could say the FWHM of MCA spectrum in any dynamic range is the walk value of TSCA in that dynamic range. In order to evaluate the constructed TSCA performance this experiment was repeated for the ORTEC TSCA. The results of this experiment for the constructed TSCA and ORTEC are shown in Figs. 7-10.

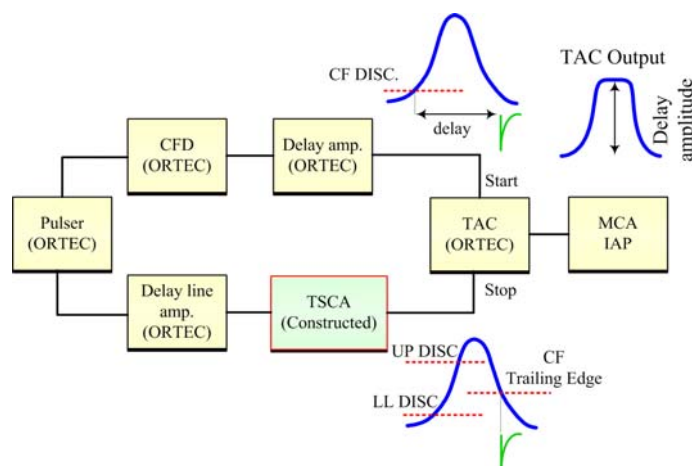


Fig. 6. Walk measurement Setup of the TSCA

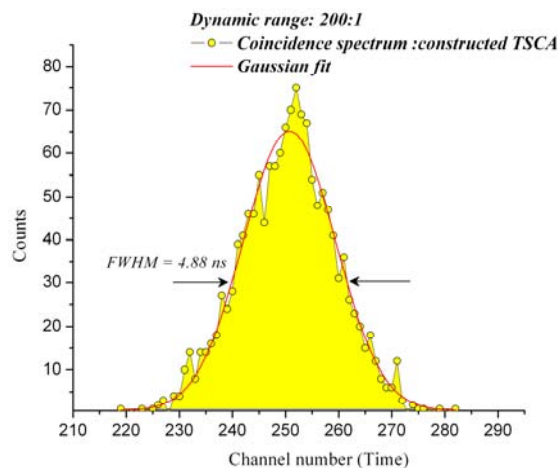


Fig. 7. Walk measurement result of constructed TSCA for 200:1 dynamic range

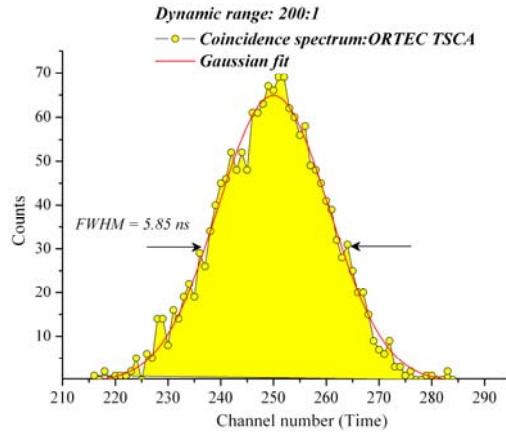


Fig. 8. Walk measurement result of ORTEC TSCA for 200:1 dynamic range

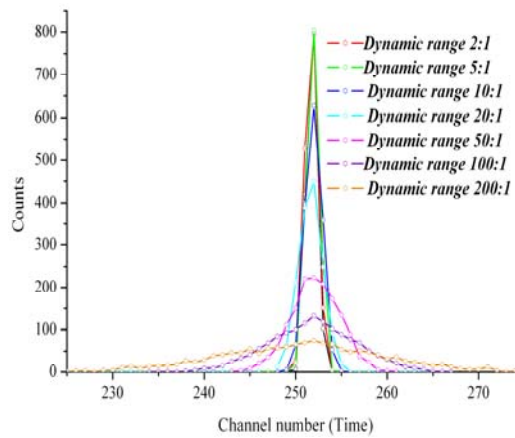


Fig. 9. Walk measurement result of constructed TSCA for 200:1, 100:1, 50:1, 20:1, 10:1 5:1 and 2:1 dynamic ranges

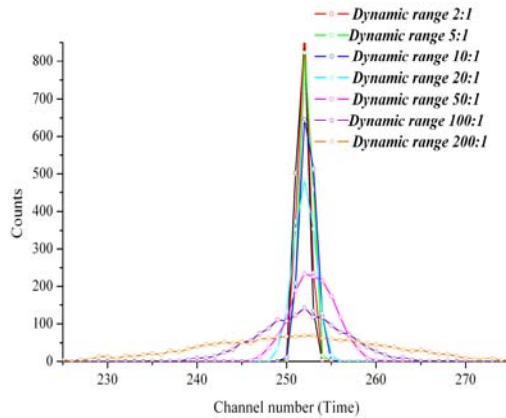


Fig. 10. Walk measurement result of ORTEC TSCA for 200:1, 100:1, 50:1, 20:1, 10:1 5:1 and 2:1 dynamic ranges

Walk of constructed TSCA is quite similar to the ORTEC one in three dynamic ranges 100:1, 50:1 and 10:1. The walk is $\leq \pm 3\text{ns}$ for the dynamic range 100:1 and $\leq \pm 2\text{ns}$ for the dynamic range 50:1 and is $\leq \pm 0.5\text{ns}$ for dynamic range 10:1. But in the 200:1 dynamic range, as shown in Figs. 7 and 8, the walk of the constructed TSCA is $\leq \pm 4.88\text{ns}$, and for ORTEC is $\leq \pm 5.85\text{ns}$ that show the better performance of constructed TSCA in extended dynamic ranges than that of ORTEC. Figs 9 and 10 show the walk variation of constructed and ORTEC TSCA's versus dynamic ranges: 200:1, 100:1, 50:1, 20:1, 10:1 5:1 and 2:1.

Pulse height analysis is the other important function of TSCA, and it is very important to be stable and precise. The nonlinearity of LLD has been measured using a set up which is shown in Fig. 11. In this set up the TSCA unit acts as a gate of MCA. In other words, any signal having an amplitude larger than the lower level discriminator of TSCA (in the integral mode of TSCA) could be recorded in MCA. So the lower level discriminator nonlinearity of TSCA could be measured by varying the lower level potentiometer and recording the MCA swapped channels. In the range of the 1024 channel of MCA, each channel equals about 9.76 mV. The swapped channel multiplied by 9.76 mV should be equal to the discriminator value read from the front panel potentiometer, therefore, any differences could be defined as a nonlinearity of the discriminator. The result of this experiment is shown in Fig. 12.

An upper level discriminator nonlinearity measurement set up similar to the lower levels set was used. But here the lower level discriminator was set to the lowest value and the upper level potentiometer value from 10 V to zero (in the normal mode of TSCA) was changed. The result of this experiment is shown in Fig. 13.

According to Figs. 12 and 13, the lower level discriminator nonlinearity for constructed TSCA is $\leq \pm 0.229\%$ of the full range and its upper level discriminator nonlinearity is $\leq \pm 0.219\%$ of the full range. Regarding these results the nonlinearity values of constructed TSCA discriminators are improved rather than the ORTEC one which have been reported in the 551 TSCA catalog ($\leq \pm 0.25$ of full range for two discriminators).

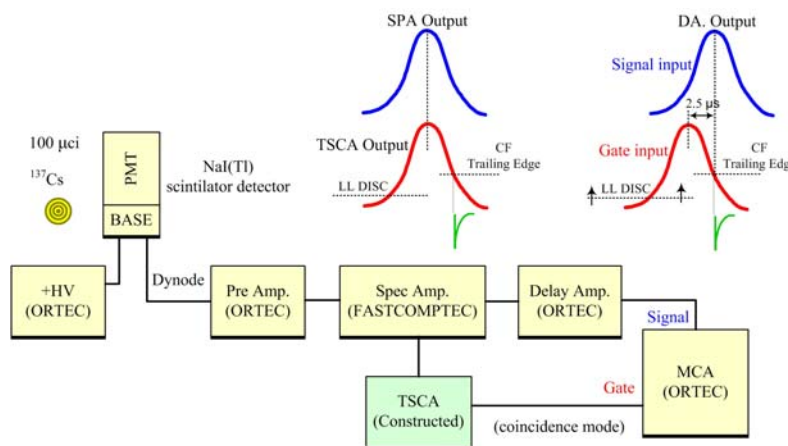


Fig. 11. Lower level discriminator nonlinearity measurement setup of TSCA

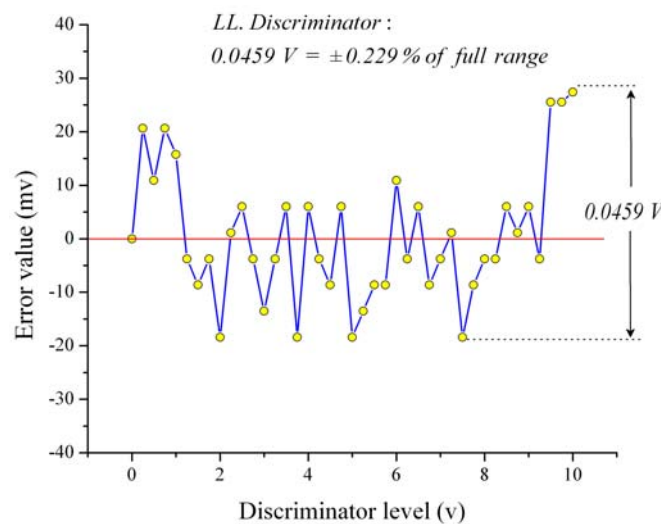


Fig. 12. Lower level discriminator nonlinearity measurement result of constructed TSCA

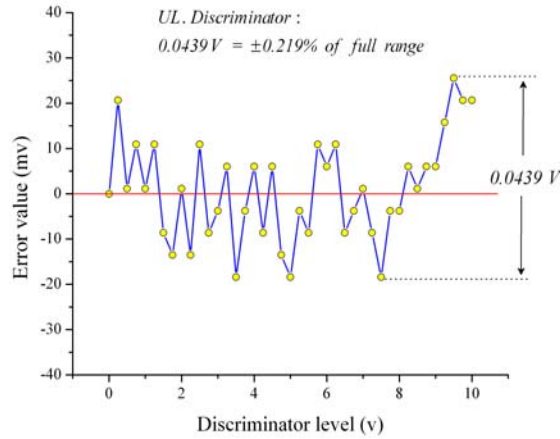


Fig. 13. Upper level discriminator nonlinearity measurement result of constructed TSCA

We used a coincidence setup using a ^{22}Na source (which emits two 511 keV coincidence gamma rays) and two separate scintillator detectors (NE-213), for the assessment of constructed TSCA performance in a real situation. This setup is shown in Fig. 14. The lower level discriminator values of TSCA's were adjusted at about 100 mV, so the corresponding dynamic range is 100:1. The resulted spectrum from this experiment for constructed TSCA's is shown in Fig. 15. This experiment was repeated using ORTEC TSCA's, and the result shown in Fig. 16.

As shown in Figs. 13 and 14, the FWHM value of coincidence spectrum by using constructed TSCA is about 1.37 ns whereas this value is about 1.57 ns in the case of using ORTEC TSCA. Therefore constructed TSCA have a better timing performance rather than similar one.

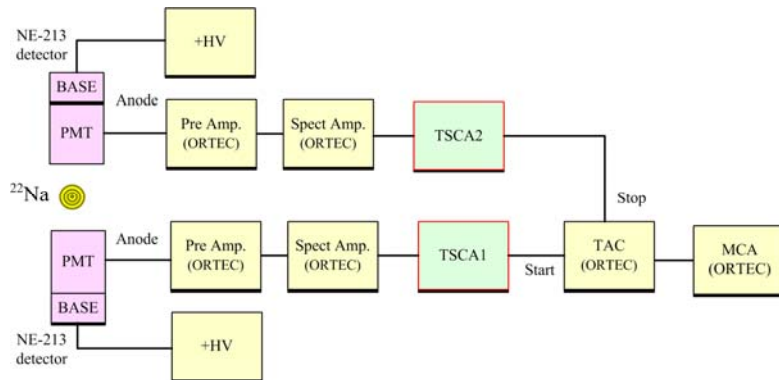


Fig. 14. Gamma-gamma Coincidence setup for ^{22}Na source by using two TSCA units

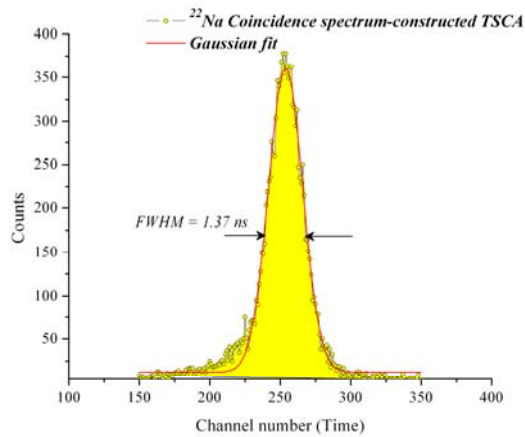


Fig. 15. Coincidence spectrum of ^{22}Na by using constructed TSCA in setup Fig 14

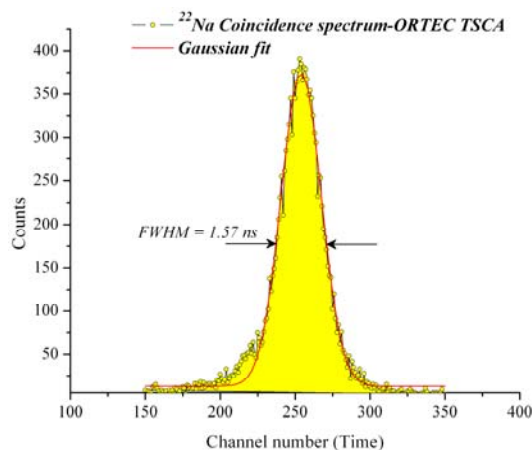


Fig. 16. Coincidence spectrum of ^{22}Na by using ORTEC TSCA in setup Fig 14

4. CONCLUSIONS

Using the constant fraction trailing edge timing method and simulation of our designed circuit by PSPICE software before implementation, an accurate and high performance TSCA in a single width NIM module has been constructed. The tests show the delay temperature instability $\leq 0.01\%$ / $^{\circ}\text{C}$ of full scale (measured by PSPICE simulation), peak detection temperature instability $\leq 0.04\%$ / $^{\circ}\text{C}$ of full scale (measured by PSPICE simulation), walk $\leq \pm 4.88\text{ns}$ in 200:1 dynamic range and discriminators nonlinearity $\leq \pm 0.23\%$ of full range. These results demonstrate that constructed TSCA outperforms other similar ones and it is, therefore well suited for time pickoff applications such as coincidence experiments.

REFERENCES

1. Okada, Y., Takahashi, T., Sato, G., Watanabe, S., Nakazawa, K., Mori, K. & Makishima, K. (2001). CdTe and CdZnTe detectors for timing measurements, *Nuclear Science Symposium Conference Record, IEEE*, 2429-2433.
2. Heinrich, B., Musiol, G. & Richter, U. (1983). Fast Analysis of Element Contents by Inelastic Scattering of Neutrons and the Method of Time Correlated Associated Particles. *Isotopes in Environmental and Health Studies*, 309-312.
3. Abbasi Davani, F., Koohi Fayegh, R., Afarideh, H., Etaati, G. R. & Aslani, G. R. (2003). Design, calibration and testing of the NRCAM fast neutron spectrometry system. *Radiat. Meas.*, 37(3), 237-245.
4. Knoll, G. F. (2000). *Radiation Detection and Measurement*. John Wiley & Sons, 659.
5. Knoll, G. F. (2000). *Radiation Detection and Measurement*. John Wiley & Sons, 659-665.
6. U.S. Patent, No. 3,714,464.
7. PSPICE Version 10.0, copyright by Cadence Design Systems, Inc.